JACS
JOURNAL OF THE AMERICAN CHEMICAL SOCIETY
Communication
pubs.acs.org/JACS

Designing a Beryllium-Free Deep-Ultraviolet Nonlinear Optical Material without a Structural Instability Problem

Sangen Zhao,[†] Lei Kang,[‡,∥] Yaoguo Shen,[†,∥] Xiaodong Wang,[§] Muhammad Adnan Asghar,[†,∥] Zheshuai Lin,*[,‡] Yingying Xu,[†,∥] Siyuan Zeng,[†] Maochun Hong,[†] and Junhua Luo*[,†]

[†]State Key Laboratory of Structural Chemistry, and Key Laboratory of Optoelectronic Materials Chemistry and Physics, Fujian Institute of Research on the Structure of Matter, Chinese Academy of Sciences, Fuzhou, Fujian 350002, China

[‡]Beijing Center for Crystal R&D, Key Lab of Functional Crystals and Laser Technology of Chinese Academy of Sciences, Technical Institute of Physics and Chemistry, Chinese Academy of Sciences, Beijing 100190, China

[§]Changchun Institute of Optics, Fine Mechanics and Physics, Chinese Academy of Sciences, Changchun 130033, China

[∥]University of Chinese Academy of Sciences, Beijing 100049, China

Supporting Information

ABSTRACT: A beryllium-free deep-ultraviolet (deep-UV) nonlinear optical (NLO) material $K_3Ba_3Li_2Al_4B_6O_{20}F$ is developed mainly by the element substitution of Be for Al and Li from $Sr_2Be_2B_2O_7$ that was considered as one of the most promising deep-UV NLO materials. $K_3Ba_3Li_2Al_4B_6O_{20}F$ preserves the structural merits of $Sr_2Be_2B_2O_7$ and thus exhibits no layering growth tendency and possesses the optical properties required for deep-UV NLO applications, including deep-UV transparency, phase-matchability, and sufficiently large second-harmonic generation (1.5 × KH_2PO_4). Furthermore, it overcomes the structural instability problem of $Sr_2Be_2B_2O_7$, which is confirmed by the obtainment of large single crystals and phonon dispersion calculations. These attributes make it very attractive for next-generation deep-UV NLO materials. The substitution of Be for Al and Li in beryllium borates provides a new opportunity to design beryllium-free deep-UV NLO materials with good performance.

Deep-ultraviolet (deep-UV) nonlinear optical (NLO) materials, which can produce coherent light of wavelengths below 200 nm, play a unique and crucial role in laser science and technology.[1] $KBe_2BO_3F_2$ (KBBF)[2] is the sole NLO material that can practically generate deep-UV coherent light by direct second-harmonic generation (SHG) process, but it contains the highly toxic element beryllium and exhibits a serious layering tendency in single-crystal growth due to its weak interlayer bonding, which have greatly limited the production and applications of KBBF. Therefore, beryllium-free deep-UV NLO materials have attracted more and more attention in recent years.[3]

To overcome the layering tendency of KBBF, Chen et al.[4] synthesized a new beryllium borate $Sr_2Be_2B_2O_7$ (SBBO) in 1995. SBBO features $[Be_2B_2O_7]_\infty$ double-layers in which the NLO-active $[BO_3]^{3-}$ groups, as like those in the $[Be_2BO_3F_2]_\infty$ single-layers in KBBF, are in coplanar and aligned arrangement, giving rise to sufficient SHG response and birefringence for deep-UV NLO applications. Furthermore, the $[Be_2B_2O_7]_\infty$ double-layers are interconnected by relatively strong Sr−O bonds (in comparison, K^+−F^- ionic bonds for KBBF), thereby greatly mitigating the layering growth tendency. Thus, SBBO has ever been considered as one of the most promising candidates for the next generation of KBBF. However, SBBO suffers a structural instability problem; as a result, the structure of SBBO has not been well solved (the structural convergence index >0.06), and large SBBO crystals of optical quality have not been obtained yet.[5]

To overcome the structural instability problem while maintaining the favorable double-layered structure of SBBO, Huang et al.[6] designed a double-layered borate in 2011, namely, $NaCaBe_2B_2O_6F$. As compared with SBBO, $NaCaBe_2B_2O_6F$ provides a more "comfortable" (or larger) space to accommodate the even smaller Na^+ cations (in comparison with Sr^{2+} cations in SBBO) inside its $[Be_2B_2O_6F]_\infty$ double-layers, which in turn stabilizes its crystal structure. Unfortunately, the Na^+ cations also make the NLO-active $[BO_3]^{3-}$ groups in an unfavorable arrangement so that $NaCaBe_2B_2O_6F$ exhibits a quite small SHG response (1/3 × KH_2PO_4 (KDP) or ∼1/4 × KBBF). Based upon the diagonal relationships of the periodic table of elements, Ye et al.[7] developed a double-layered borate $BaAl_2B_2O_7$ by the substitution of the toxic Be of SBBO for relatively large Al atoms. Nevertheless, the instability problem still occurs in $BaAl_2B_2O_7$, indicating the substitution of Be for Al cannot create a sufficiently "comfortable" space in the resulting double-layers to accommodate large Ba^{2+} cations.

Because Li atoms often four-coordinate with O/F atoms like Be atoms while having markedly larger ionic radii than the latter, we attempted to further substitute Be of SBBO for Al and Li to create SBBO-like double-layered borates but without structural instability. A hypothesized formula can be derived as $A_3B_3C_6B_6O_{18}O_xF_{3-x}$ when the double-layered structures are viewed as a sum of five parts, namely, A-, B-, and C-site cations, $[BO_3]^{3-}$ anions as well as O^{2-}/F^- bridges:

$$3Sr_2Be_2B_2O_7\text{: } 3Sr^{2+} + 3Sr^{2+} + 6Be^{2+} + 6[BO_3]^{3-} + 3O^{2-}$$

$$3NaCaBe_2B_2O_6F\text{: } 3Na^+ + 3Ca^{2+} + 6Be^{2+} + 6[BO_3]^{3-} + 3F^-$$

Received: January 13, 2016
Published: February 18, 2016

DOI: 10.1021/jacs.6b00436
J. Am. Chem. Soc. 2016, 138, 2961−2964

$$A_3B_3C_6B_6O_{18}O_xF_{3-x}: 3A^+ + 3B^{2+} + \{yLi^+ + (6-y)Al^{3+}\} + 6[BO_3]^{3-} + \{xO^{2-} + (3-x)F^-\}$$

Taking charge balance into account, a possible formula can be deduced, viz. $A_3B_3Li_2Al_4B_6O_{20}F$. On this basis, we successfully synthesized a targeted beryllium-free borate, $K_3Ba_3Li_2Al_4B_6O_{20}F$ (**I**).

Polycrystalline samples of **I** were synthesized by the traditional solid-state reaction techniques based on the following reaction:

$$3K_2CO_3 + 6BaCO_3 + Li_2CO_3 + 2LiF + 4Al_2O_3 + 12H_3BO_3 = 2K_3Ba_3Li_2Al_4B_6O_{20}F + 9CO_2 + 18H_2O$$

The experimental powder X-ray diffraction (XRD) pattern matches well with the one calculated from single-crystal XRD analysis (see Figure S1 in the Supporting Information). The thermal stability of **I** was investigated by the differential scanning calorimetric analysis. As shown in Figure S2, there is a sharp endothermic peak around 874 °C in the heating curve and no exothermic peak in the cooling curve, indicating that **I** melts incongruently around 874 °C. Therefore, large crystals of **I** should be grown using flux method below 874 °C. In this work, we grew **I** crystals using a Li_2O-BaF_2-B_2O_3 flux through the top-seeded growth method. As shown in Figure 1a, the as-grown single crystal is of block shape ($10 \times 5 \times 3$ mm^3) with a thickness of about 5 mm in the *c* direction. It should be emphasized that this crystal was just grown by our preliminary experiments, and thus it can be anticipated that even thicker crystals would be obtained by optimizing the growth conditions. In contrast, the thickest KBBF crystal known to date only has a thickness of 3.7 mm in the *c* direction.[8] Therefore, we can conclude that the **I** crystal overcomes the layering growth tendency.

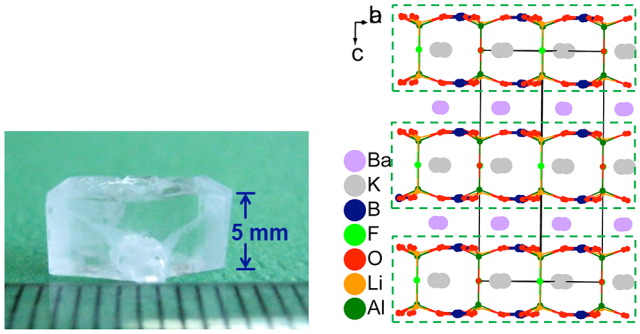

Figure 1. (a) As-grown single crystal of **I**. Thickness in the *c* direction is indicated. (b) Crystal structure of **I**. The $[Li_2Al_4B_6O_{20}F]_\infty$ double-layers are indicated by dashed green rectangles.

The crystal structure of **I** was determined by single-crystal XRD analysis. **I** crystallizes in the hexagonal crystal system with an asymmetric space group of $\bar{P}62c$ (detailed crystallographic data see Tables S1–S4). As shown in Figure 1b, its crystal structure is composed of $[Li_2Al_4B_6O_{20}F]_\infty$ double-layers, which stack along the *c* axis with Ba^{2+} cations residing in the interlayer space to serve as interlayer connectors (via Ba–O bonds). K^+ cations occupy the cavities of the $[Li_2Al_4B_6O_{20}F]_\infty$ double-layers to maintain charge balance. Each $[Li_2Al_4B_6O_{20}F]_\infty$ double-layer consists of two alveolate $[LiAl_2B_3O_{10}F]_\infty$ single-layers which are tightly connected to each other via the bridged O/F atoms. AlO_4/LiO_3F tetrahedra and $[BO_3]^{3-}$ triangles are arranged in a trigonal pattern, endowing the $[BO_3]^{3-}$ groups coplanar and aligned arrangement in $[LiAl_2B_3O_{10}F]_\infty$ single-layers (Figure S3). This structural feature is favorable to generate sufficient SHG response and birefringence for deep-UV NLO applications, just like the cases of KBBF[2a] and SBBO.[4]

The O–B–O angles are in the range of 118.8(9)–121.2(9)° with a mean value of about 120°, indicating that the $[BO_3]^{3-}$ triangle is nearly planar. As shown in Table S4, all the bond distances in **I** are normal. The results of bond valence calculations[9] (B, 3.03; Al1, 3.25; Al2, 3.12; Li1, 1.16; K, 0.74; Ba, 1.85; O, −1.81 to −2.10; F, −1.16) indicate that the K, Ba, Li, Al, B, O, and F atoms are in the expected oxidation states of +3, +3, +3, +1, +1, +2, −2, and −1, respectively. The inductively coupled plasma element analysis gave a molar ratio of K:Ba:Li:Al:B = 2.79:3.10:1.91:4.16:6.28, which is in good agreement with the formula sum deduced by single-crystal XRD analysis.

The structural evolution, from KBBF, SBBO, and $NaCaBe_2B_2O_6F$ to **I**, is illustrated in Figure 2. All these borates feature layered structural units composed of $[BO_3]^{3-}$ triangles and tetrahedra (BeO_3F for KBBF, BeO_4 for SBBO, BeO_3F for $NaCaBe_2B_2O_6F$, and AlO_4 and LiO_3F for **I**). Except KBBF with single-layers, the other three borates have similar double-layers. Meanwhile, as compared with KBBF that exhibits weak interlayer bonding (K^+–F^- ionic bonds), the interlayer bonding for the other three borates (Sr–O bonds for SBBO, Ca–O bonds for $NaCaBe_2B_2O_6F$, and Ba–O bonds for **I**) is evidently reinforced, thereby resulting in no layering growth tendency for their crystals. Notably, the arrangement of $[BO_3]^{3-}$ groups is different in the four borates. For $NaCaBe_2B_2O_6F$, the $[BO_3]^{3-}$ groups are in an unfavorable arrangement (not coplanar, aligned in different orientations) so that the resulting SHG response is quite small (1/3 × KDP or ~1/4 × KBBF).[6] In

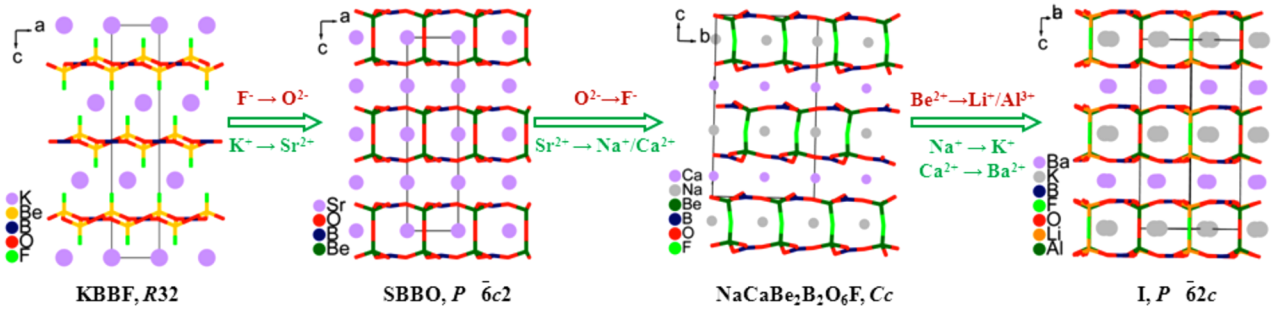

Figure 2. Structural evolution from KBBF, SBBO, and $NaCaBe_2B_2O_6F$ to **I**. Element substitution is indicated for these borates.

DOI: 10.1021/jacs.6b00436
J. Am. Chem. Soc. 2016, 138, 2961–2964

contrast, the $[BO_3]^{3-}$ groups in KBBF, SBBO, and **I** are coplanar and aligned in a similar, favorable manner, indicating that they will share the favorable NLO properties. Moreover, the bridged Li−F (1.889 Å) and Al−O bonds (1.706−1.715 Å) for **I** are longer than those of the bridged Be−F bonds (1.681 Å) for $NaCaBe_2B_2O_6F$ and especially the bridged Be−O bonds (1.632 Å) for SBBO. These bond distances endow the $[Li_2Al_4B_6O_{20}F]_\infty$ double-layers in **I** a "comfortable" space to accommodate even the largest K^+ cations (as compared with the Sr^{2+} in SBBO and Na^+ in $NaCaBe_2B_2O_6F$). As a result, **I** overcomes the structural instability problem inherent in the structure of SBBO; the structural converge factor for **I** is 0.0220, much smaller than that of SBBO (>0.065);[4] in our preliminary crystal growth attempts, a large-sized **I** single crystal was obtained (Figure 1a), which provides a solid evidence for the structural stability of **I**.

Deep-UV transmission spectrum was collected at room temperature on a McPherson VUVas2000 spectrophotometer in the range of 120−220 nm. A transparent **I** crystal with a thickness of about 0.5 mm was used for the measurement without polishing. As shown in Figure 3a, **I** is deep-UV

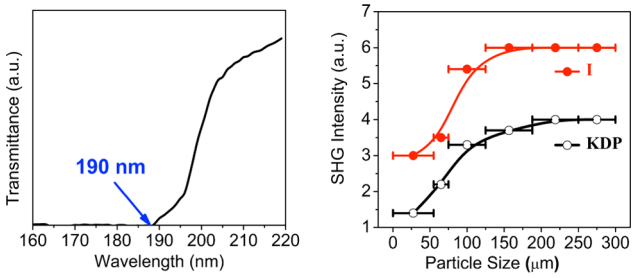

Figure 3. (a) Deep-UV transmission spectrum of **I**. (b) SHG intensity vs particle size curves at 1064 nm. The solid curves in (b) are drawn to guide the eyes and are not fits to the data.

transparent down to about 190 nm. Obviously, this measurement on single crystal provides more accurate results than the diffuse reflectance method on powders. Since **I** crystallizes in an asymmetric space group, it is expected to be SHG-active. We carried out powder SHG measurements by the Kurtz−Perry method[10] with an incident laser of 1064 nm. As shown in Figure 3b, the SHG intensities for **I** increase with increasing particle sizes before they reach the maximum independent of the particle sizes. According to the rule proposed by Kurtz and Perry,[10] **I** is a phase-matching NLO material. The SHG efficiency for **I** is about 1.5 times that of KDP at the same particle sizes of 250−300 μm. Such a SHG response is large enough for deep-UV NLO applications (for KBBF it is ~1.24 × KDP).[11] It is also comparable to those of the layered beryllium borates, such as $RbBe_2B_3O_7$ (0.79 × KDP),[12] $NaBeB_3O_6$ (1.60 × KDP),[12] $Na_2CsBe_6B_5O_{15}$ (1.17 × KDP),[1c] as well as $Na_2Be_4B_4O_{11}$ (1.3 × KDP) and $LiNa_5Be_{12}B_{12}O_{33}$ (1.4 × KDP).[1a]

We performed the first-principle calculations on the electronic structrue and optical properties of **I** by the plane-wave pseudopotential method implemented in the CASTEP package.[13] The density of states and partial density of states projected on the constitutional atoms (see Figure S4) demonstrate that the $[BO_3]^{3-}$ group determines the SHG response and optical birefringence in crystal **I**, whereas the K^+, Li^+, Ba^{2+}, and Al^{3+} cations make a negligibly small contribution. The SHG coefficients (d_{ij}) were calculated by the formula developed by Lin et al.[14] Under the restriction of Kleinman's symmetry,[15] **I** has only one nonzero independent SHG coefficient owing to its $\bar{P}62c$ space group. The calculated value is d_{22} = −0.48 pm/V, which is consistent with result of the powder SHG tests. In addition, the calculated linear refractive indices for **I** (Figure S5) reveal that the crystal has a moderate birefringence, i.e., Δn = 0.052 at λ = 532 nm, which is consistent with the experimentally phase-matching behavior and its layered crystal structure.

To investigate the structural stability, we adopted the linear response method[16] to obtain the phonon dispersion of SBBO, $NaCaBe_2B_2O_6F$, and **I** (see Figure 4a−c, respectively). It is

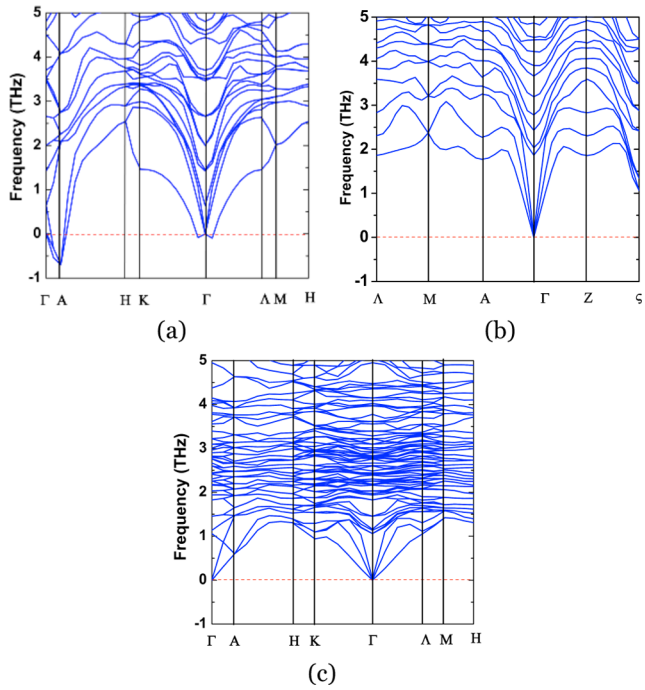

Figure 4. Phonon dispersion of (a) SBBO, (b) $NaCaBe_2B_2O_6F$, and (c) **I**.

well-known that the lattice vibration properties can be deduced from the phonon dispersion which intrinsically characterizes the interatomic interaction. The negative (imaginary) phonon eigenvalues indicate that the interatomic forces are not attractive at some reciprocal lattice points, and thus the crystal structure is not kinetically stable.[17] Clearly, for SBBO the imaginary phonon modes appear in the vicinity of the high symmetry points A and Γ in the Brillouin zone, which means that the SBBO structure is not in a kinetically stable state. In comparison, for $NaCaBe_2B_2O_6F$ and **I** the eigenvalues for all phonon modes are positive, thus confirming their structural stability theoretically. From the point of view of crystal structure, the element substitution of Be for Al and Li makes the lattice of **I** more "comfortable" to accommodate the relatively large K^+ cations, resulting in the structure of **I** overcoming the instability problem of the SBBO structure.

In summary, we have rationally designed a new beryllium-free borate $K_3Ba_3Li_2Al_4B_6O_{20}F$ (**I**) by the substitution of Be for Al and Li from SBBO. This borate features a double-layered structure that preserves the structural merits of KBBF and SBBO. As a result, **I** exhibits the optical properties required for deep-UV NLO applications, including deep-UV transparency,

DOI: 10.1021/jacs.6b00436
J. Am. Chem. Soc. 2016, 138, 2961−2964

phase-matchability, and sufficiently large SHG response of 1.5 × KDP. Meanwhile, we have grown a large-sized single crystal of **I** with a thickness of about 5 mm in the *c* direction, demonstrating **I** has no layering single-crystal growth tendency. Furthermore, **I** eliminates the structural instability of SBBO, which is confirmed by the small structural converge factor, obtainment of large-sized **I** single crytal, and phonon dispersion calculations. These attributes make **I** an attractive candidate for the next-generation deep-UV NLO materials. Moreover, the substitution of Be for Al and Li in beryllium borates provides a new opportunity to design beryllium-free deep-UV NLO materials with good performance.

■ ASSOCIATED CONTENT

Supporting Information

The Supporting Information is available free of charge on the ACS Publications website at DOI: 10.1021/jacs.6b00436.

Experimental details and data; deposition number CCDC 1444282 for **I** (PDF)
Crystallographic data (CIF)

■ AUTHOR INFORMATION

Corresponding Authors

*jhluo@fjirsm.ac.cn
*zslin@mail.ipc.ac.cn

Notes

The authors declare no competing financial interest.

■ ACKNOWLEDGMENTS

This work was financially supported by NSFC of China (21525104, 91422301, 11474292, 21373220, 51502288, 51502290, 21571178) and 863 Program of China (2015AA034203). S.Z. is grateful for the support from the NSF for Distinguished Young Scholars of Fujian Province (2016J0103), Chunmiao Project of Haixi Institute of Chinese Academy of Sciences (CMZX-2015-003) and Youth Innovation Promotion of CAS (2016274).

■ REFERENCES

(1) (a) Wu, H. P.; Yu, H. W.; Yang, Z. H.; Hou, X. L.; Su, X.; Pan, S. L.; Poeppelmeier, K. R.; Rondinelli, J. M. *J. Am. Chem. Soc.* **2013**, *135*, 4215. (b) Huang, H. W.; Yao, J. Y.; Lin, Z. S.; Wang, X. Y.; He, R.; Yao, W. J.; Zhai, N. X.; Chen, C. T. *Angew. Chem., Int. Ed.* **2011**, *50*, 9141. (c) Wang, S. C.; Ye, N. *J. Am. Chem. Soc.* **2011**, *133*, 11458. (d) Huang, H. W.; Liu, L. J.; Jin, S. F.; Yao, W. J.; Zhang, Y. H.; Chen, C. T. *J. Am. Chem. Soc.* **2013**, *135*, 18319. (e) Wu, H. P.; Yu, H. W.; Pan, S. L.; Huang, Z. J.; Yang, Z. H.; Su, X.; Poeppelmeier, K. R. *Angew. Chem., Int. Ed.* **2013**, *52*, 3406. (f) Zhao, S. G.; Gong, P. F.; Luo, S. Y.; Bai, L.; Lin, Z. S.; Ji, C. M.; Chen, T. L.; Hong, M. C.; Luo, J. H. *J. Am. Chem. Soc.* **2014**, *136*, 8560. (g) Zhao, S. G.; Gong, P. F.; Luo, S. Y.; Bai, L.; Lin, Z. S.; Tang, Y. Y.; Zhou, Y. L.; Hong, M. C.; Luo, J. H. *Angew. Chem., Int. Ed.* **2015**, *54*, 4217.

(2) (a) Xia, Y. N.; Chen, C. T.; Tang, D. Y.; Wu, B. C. *Adv. Mater.* **1995**, *7*, 79. (b) Cyranoski, D. *Nature* **2009**, *457*, 953.

(3) (a) Zhao, S. G.; Gong, P. F.; Bai, L.; Xu, X.; Zhang, S. Q.; Sun, Z. H.; Lin, Z. S.; Hong, M. C.; Chen, C. T.; Luo, J. H. *Nat. Commun.* **2014**, *5*, 4019. (b) Zhao, S. G.; Gong, P. F.; Luo, S. Y.; Liu, S. J.; Li, L. N.; Asghar, M. A.; Khan, T.; Hong, M. C.; Lin, Z. S.; Luo, J. H. *J. Am. Chem. Soc.* **2015**, *137*, 2207. (c) Yu, H.; Zhang, W.; Young, J.; Rondinelli, J. M.; Halasyamani, P. S. *Adv. Mater.* **2015**, *27*, 7380. (d) Tran, T. T.; He, J. G.; Rondinelli, J. M.; Halasyamani, P. S. *J. Am. Chem. Soc.* **2015**, *137*, 10504. (e) Yu, P.; Wu, L. M.; Zhou, L. J.; Chen, L. *J. Am. Chem. Soc.* **2014**, *136*, 480.

(4) Chen, C. T.; Wang, Y. B.; Wu, B. C.; Wu, K. C.; Zeng, W. L.; Yu, L. H. *Nature* **1995**, *373*, 322.

(5) (a) Chen, C. T. *J. Synth. Cryst.* **2001**, *30*, 36. (b) Meng, X. Y.; Wen, X. H.; Liu, G. L. *J. Korean Phys. Soc.* **2008**, *52*, 1277.

(6) Huang, H. W.; Yao, J. Y.; Lin, Z.; Wang, X. Y.; He, R.; Yao, W. J.; Zhai, N. X.; Chen, C. T. *Chem. Mater.* **2011**, *23*, 5457.

(7) Ye, N.; Zeng, W. R.; Wu, B. C.; Huang, X. Y.; Chen, C. T. *Z. Kristallogr. - New Cryst. Struct.* **1998**, *213*, 452.

(8) Wang, X.; Yan, X.; Luo, S.; Chen, C. *J. Cryst. Growth* **2011**, *318*, 610.

(9) (a) Brown, I. D.; Altermatt, D. *Acta Crystallogr., Sect. B: Struct. Sci.* **1985**, *41*, 244. (b) Brese, N. E.; O'keeffe, M. *Acta Crystallogr., Sect. B: Struct. Sci.* **1991**, *47*, 192.

(10) Kurtz, S. K.; Perry, T. T. *J. Appl. Phys.* **1968**, *39*, 3798.

(11) Chen, C. T.; Wang, G. L.; Wang, X. Y.; Xu, Z. Y. *Appl. Phys. B: Lasers Opt.* **2009**, *97*, 9.

(12) Wang, S. C.; Ye, N.; Li, W.; Zhao, D. *J. Am. Chem. Soc.* **2010**, *132*, 8779.

(13) (a) Kohn, W.; Sham, L. J. *Phys. Rev.* **1965**, *140*, A1133. (b) Payne, M. C.; Teter, M. P.; Allan, D. C.; Arias, T. A.; Joannopoulos, J. D. *Rev. Mod. Phys.* **1992**, *64*, 1045. (c) Clark, S. J.; Segall, M. D.; Pickard, C. J.; Hasnip, P. J.; Probert, M. J.; Refson, K.; Payne, M. C. *Z. Kristallogr. - Cryst. Mater.* **2005**, *220*, 567.

(14) (a) Lin, J.; Lee, M. H.; Liu, Z. P.; Chen, C. T.; Pickard, C. J. *Phys. Rev. B: Condens. Matter Mater. Phys.* **1999**, *60*, 13380. (b) Lin, Z. S.; Lin, J.; Wang, Z. Z.; Wu, Y. C.; Ye, N.; Chen, C. T.; Li, R. K. *J. Phys.: Condens. Matter* **2001**, *13*, R369.

(15) Kleinman, D. A. *Phys. Rev.* **1962**, *126*, 1977.

(16) Baroni, S.; de Gironcoli, S.; Dal Corso, A.; Giannozzi, P. *Rev. Mod. Phys.* **2001**, *73*, 515.

(17) Yao, Y.; Tse, J. S.; Sun, J.; Klug, D. D.; Martonak, R.; Iitaka, T. *Phys. Rev. Lett.* **2009**, *102*, 229601.

DOI: 10.1021/jacs.6b00436
J. Am. Chem. Soc. 2016, 138, 2961−2964